International Journal of Solids and Structures 230–231 (2021) 111162

Contents lists available at ScienceDirect

International Journal of Solids and Structures

journal homepage: www.elsevier.com/locate/ijsolstr

Size-dependent bending modulus of fibre composite laminates comprising unidirectional plies

Nastaran Nourmohammadi, Noel P. O'Dowd *, Paul M. Weaver

School of Engineering, Bernal Institute, University of Limerick, Limerick V94 T9PX, Ireland

ARTICLE INFO

Article history:
Received 30 October 2020
Received in revised form 7 June 2021
Accepted 5 July 2021
Available online 17 July 2021

Keywords:
Heterogeneity
Composite ply
Bending stiffness
Laminate
Size effect
Effective bending modulus

ABSTRACT

Heterogeneous materials can show size-dependent behaviour in which the bending modulus depends on sample size. In fibre composite materials the interaction between fibre and matrix can lead to such a size effect.Then the effective modulus calculated by the rule of mixtures can either underestimate or overestimate the bending modulus of the laminate, depending on the fibre/matrix material mismatch, the microstructural morphology (fibre distribution) and the laminate thickness. In this work, the bending behaviour of a laminate comprising unidirectional fibre composite plies is considered using Euler-Bernoulli beam theory and the influence of size on the bending modulus is investigated. The effective bending modulus of each ply is calculated and used to formulate the overall bending modulus of the laminate. The results show that the laminate bending modulus depends on the number of plies, the number of fibres through the thickness of each ply, the fibre spacing and radius, and the mismatch of fibre and matrix material properties in each ply. Our analysis shows that accounting for the ply microstructure (fibre spacing and radius and number of fibres per ply) can lead to a 10% difference in the predicted bending modulus in a three ply laminate, when there are less than four fibres through the thickness in each ply.

1. Introduction

Heterogeneous materials can show size dependent behaviour under bending in which the effective modulus depends on size (Nourmohammadi et al., 2020; Wheel et al., 2015). The term 'positive size effect' has been used when the modulus increases with decreasing size and 'negative size effect' for the case when modulus decreases with decreasing size. Materials such as polymeric foams (Lakes, 1983), lattices (Bažant and Christensen, 1972), and materials with spherical voids in a matrix (Yang and Lakes, 1982), have been shown to have a positive size effect under bending. The bending behaviour of heterogeneous media can be modelled through Cauchy elasticity theory in which the contribution of each component on bending stiffness is analysed separately and simply added together to obtain the total stiffness. In previous work (Nourmohammadi et al., 2020), the bending stiffness of fibres and matrix through thickness of a thin-ply composite with uniform fibre spacing was calculated separately using Euler-Bernoulli beam theory and accumulated to achieve the total stiffness. As analysing heterogeneous media is computationally expensive, it is desirable to provide an equivalent homogenised model. Work done by Bigoni and Drugan (2007) showed that the elastic strain energy of a heterogeneous representative volume element (RVE) under uniform loading is equal to that calculated using the effective material properties from standard homogenised Cauchy methods. However, when loading is no longer uniform, a mismatch in elastic strain energy calculated from the two models arises. To address this problem, an equivalent model using generalised continuum models is proposed in which additional material constituents account for the difference in the strain energies. The concept of the generalised continuum was initially introduced by the Cosserat brothers in which a series of substructures in classical Cauchy media rotate independently from each other (Cosserat, 1970). Micropolar and modified couple stress theories (Eringen, 1972; Yang et al., 2002; Park and Gao, 2006) are two widely used generalised continuum models that represent a heterogeneous Euler-Bernoulli beam under bending. The simplicity of their constitutive equations is desirable as there is just one length scale parameter responsible for the size effect. In other words, in the classical homogenisation methods, the length scale parameter is essentially zero (Ma et al., 2011). In the micropolar theorem, rotations and micro-moments are additional degrees of freedom to translations and forces. In the modified couple stress theorem, the couple stress tensor is symmetric and there are equilibrium expressions for

* Corresponding author.
E-mail addresses: Nastaran.Nour@ul.ie (N. Nourmohammadi), Noel.ODowd@ul.ie (N.P. O'Dowd), Paul.Weaver@ul.ie (P.M. Weaver).

https://doi.org/10.1016/j.ijsolstr.2021.111162
0020-7683/

List of Symbols

d_k	Fibre spacing in ply k
l_k	Distance from neutral axis of ply k to laminate neutral axis
r_k	Fibre radius in ply k
t	Laminate thickness
t_k	Thickness of ply k
v_{fk}	Fibre volume fraction ratio of ply k
w	Width of the laminate
α_k	Dimensionless geometry parameter for ply k, r_k/d_k
β_k	Dimensionless material mismatch ratio for ply k, E_{fk}/E_{mk}
κ	Laminate curvature
λ_k	Ratio of fibre spacing in ply k to fibre spacing in ply 1
A_k	Cross sectional area of ply k
D^{lam}	Laminate bending stiffness
D_k	Bending stiffness of ply k with respect to the laminate neutral axis
E_{fk}	Elastic modulus of fibre for ply k
E_{mk}	Elastic modulus of matrix for ply k
$\bar{E}_k$	Effective tensile modulus of ply k using the rule of mixtures
$\hat{E}_{bk}$	Effective bending modulus of ply k with respect to its neutral axis
$\tilde{E}_{bk}$	Effective bending modulus of ply k with respect to the laminate's neutral axis
$\hat{E}_b^{lam}$	Effective bending modulus of a laminate
$\tilde{E}_b^{lam}$	Effective bending modulus of a laminate using homogenised ply properties
$\bar{E}^{lam}$	Effective tensile modulus of a laminate based on the rule of mixtures
E_{fc}	Elastic modulus of carbon fibre
E_{fg}	Elastic modulus of glass fibre
I^{lam}	Second moment of area of a homogenised laminate
I_k	Second moment of area of homogenised ply k
M	Bending moment
N_k	Number of fibres in ply k
P	$2P$ even number of plies and $2P+1$ odd number of plies in a laminate
R	Relative difference between bending modulus of laminate and modulus from rule of mixtures
R_p	Relative difference between bending modulus and modulus from rule of mixtures of a ply

moments as well as forces that arise at a material point. Both micropolar (Bigoni and Drugan, 2007) and the modified couple stress theorem (Park and Gao, 2006) contribute more strain energy than that calculated using standard Cauchy elasticity. As a result, they only capture a positive size effect in which material becomes stiffer with decreasing size. In this work, the formulation of a micropolar Euler-Bernoulli beam model (Beveridge et al., 2013) is used in which there is just one length scale parameter. In this model, three-point bending analysis of a beam with a rectangular cross-section is performed which is the simplification of previous work (Lakes, 1995) in which all out-of-plane effects were considered. As a result, both micropolar and modified couple stress theorems are indistinguishable from each other. In previous work (Nourmohammadi et al., 2020), the bending characteristic length was shown to be defined only for the case when fibres are more compliant than the matrix. Finally, the calculated bending characteristic length can be used to define the new constitutive parameters of the micropolar theorem.

Current work focuses on modelling the bending behaviour of composite materials. The heterogeneity innate to these materials not only arises because of the mismatch of fibre/matrix material and geometric properties but also due to the arrangement of fibres in the matrix and distribution of voids. In literature, the most prevalent RVE shapes are hexagonal or square (Keane et al., 2008). By having a hexagonal array, i.e. fibre centres are located on an equilateral triangular grid, higher volume fractions can be achieved. The maximum V_f for a rectangular array is 78.5%, while the maximum for a triangular array is 90.3%. Studies by Adams and Tsai (1969) have shown that under transverse loading, for the same volume fraction, the elastic modulus is higher for a square array than for a hexagonal (triangular) array. Such information is not available in the literature for longitudinal loading, as examined here, so without analysing the particular case it is difficult to speculate on the expected trend. This will be examined in future work. In addition the mechanical response under bending differs due to the change of fibre arrangement from hexagonal to square RVEs.

In previous work (Nourmohammadi et al., 2020), the bending behaviour of a thin-ply composite with a square fibre array of uniform spacing (due to its relative simplicity in the modelling) was investigated. We showed that size effects arising from the bending of a fibre reinforced composite ply can be described using Euler-Bernoulli beam theory. It was shown that the bending modulus depends on the geometry ratio, $\alpha = r/d$, where r is fibre radius and d is fibre spacing, the material mismatch ratio, $\beta = E_f/E_m$, where E_f and E_m are fibre and matrix elastic modulus, respectively, and N, the number of fibres through the thickness of the ply. Finite element (FE) validation of the results was achieved by modelling an RVE under pure bending and then subjecting it to periodic boundary conditions. An RVE was modelled and the effective bending modulus was calculated. Results showed that FE predictions and analytical solutions were in close agreement.

Wheel et al. (2015), examined a problem focusing on the bending stiffness of a symmetric laminate comprising plies with two different moduli, without considering the ply microstructure. Their results showed that if the outer ply (located furthest from the neutral axis of the laminate) has the higher modulus a positive size effect results (laminate modulus increasing with decreasing size) while a negative size effect is predicted if the outer ply has the lower modulus. In this work, the bending behaviour of a symmetric laminate, composed of an arbitrary number of unidirectional composite plies, is studied, extending our previous work (Nourmohammadi et al., 2020), which examined a single ply. The effect of material and geometry properties of the individual plies on the overall laminate response is considered, particularly in relation to size effects and the results are compared to that of Wheel et al. (2015).

2. Formulation of effective bending modulus of a laminate

A laminate of width, w, length, l, and thickness, t, under bending moment, M, about the X_2 axis, is considered, as shown in Fig. 1. The laminate is symmetric, with either an even or odd number of unidirectional plies, noting that each ply can have an even or odd number of circular cylindrical fibres through the thickness. For simplicity, the case of an even number of plies and an even number of fibres is presented in the following. Details of the calculations for an odd number of plies and an odd number of fibres are provided in Appendix A. The cross-section of the laminate is shown in Fig. 2(a).

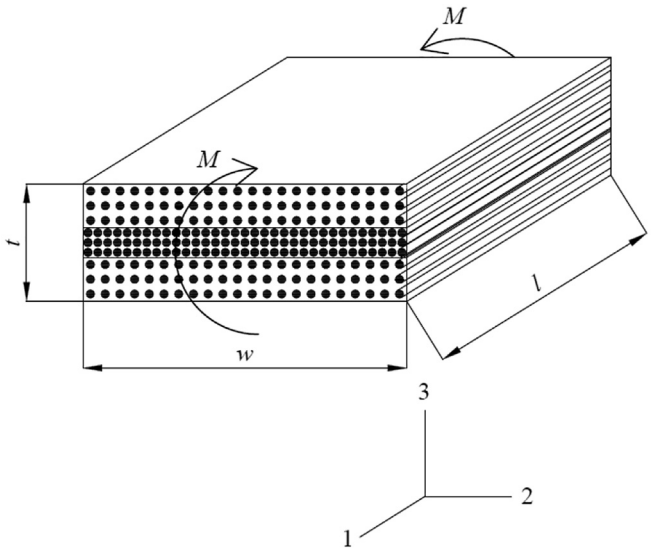

Fig. 1. Centro-symmetric laminate made up of unidirectional plies under pure bending moment, M.

Ply k has thickness t_k and lever arm l_k, which is the distance between the neutral axis of the ply (the a-axis in Fig. 2)) and the neutral axis of the laminate (the b-axis in Fig. 2(a)). The cross-section of a ply is shown in Fig. 2(b). Each ply has N_k fibres through the thickness in a rectangular array with fibre spacing d_k and fibre radius r_k. The ply thickness, $t_k = N_k d_k$. For each ply we define the geometry ratio $\alpha_k = r_k/d_k$ and the material mismatch ratio $\beta_k = E_{fk}/E_{mk}$, where E_{fk} and E_{mk} are the elastic modulus of fibre and matrix, respectively. Note that the fibre volume fraction ratio, $v_{fk} = \pi\alpha_k^2$.

From Euler-Bernoulli beam theory, the relation between moment, M, and curvature, κ, of the laminate shown in Fig. 1 is:

$$M = D^{lam}\kappa, \tag{1}$$

where D^{lam} is the bending stiffness of the laminate and the curvature, κ, is the second derivative of deflection, u_3, with respect to position x_1 along the beam,

$$\kappa = \frac{d^2u_3}{dx_1^2}. \tag{2}$$

The effective bending modulus $\hat{E}_b^{lam}$ of the laminate is defined as

$$\hat{E}_b^{lam} = \frac{D^{lam}}{I^{lam}}, \tag{3}$$

where I^{lam} is the second moment of area of the homogenised laminate,

$$I^{lam} = \frac{wt^3}{12}, \tag{4}$$

where thickness, t, for a laminate with an even number of plies, $2P$, is:

$$t = 2\sum_{k=1}^{P} t_k = 2\sum_{k=1}^{P} N_k d_k. \tag{5}$$

Defining λ_k as the fibre spacing ratio of ply k with respect to the first ply,

$$\lambda_k = \frac{d_k}{d_1}, \tag{6}$$

Eq. (5) can be rewritten as,

$$t = 2d_1\sum_{k=1}^{P} N_k\lambda_k. \tag{7}$$

and the second moment of area of the laminate, I^{lam}, can be written as,

$$I^{lam} = \frac{2wd_1^3}{3}\sum_{k=1}^{P} N_k^3\lambda_k^3, \tag{8}$$

noting that $\lambda_1 = 1$. We seek to write the effective bending modulus of the laminate $\hat{E}_b^{lam}$ in Eq. (3), in terms of the properties of the indi-

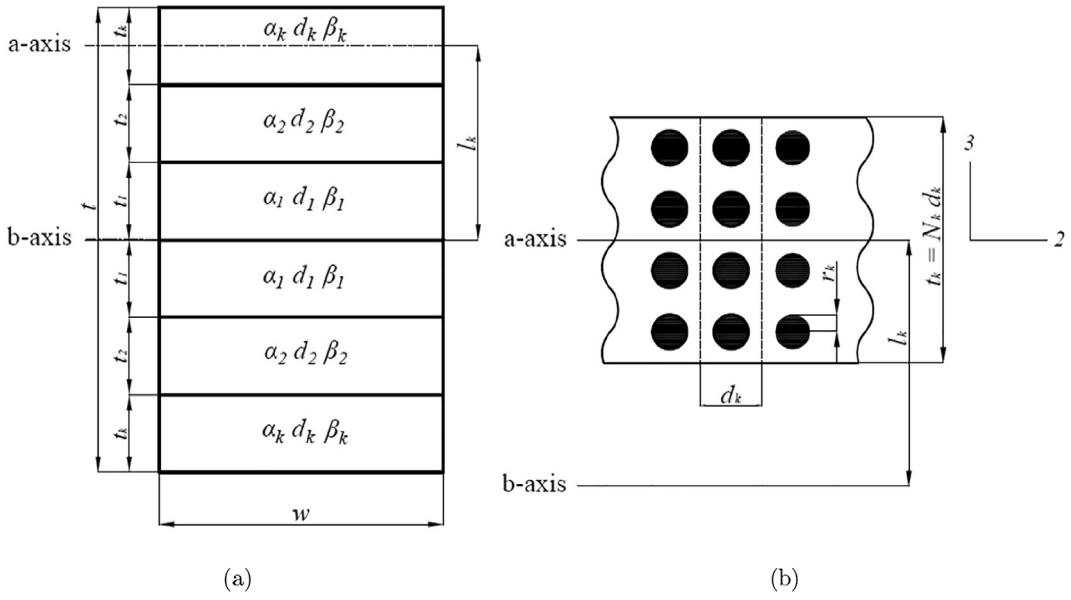

Fig. 2. Configuration of plies in the laminate and fibres in ply k with width of w and thickness of t_k: (a) Laminate with $2P$ even number of plies; (b) Ply with N_k even number of fibres.

vidual plies. Following Nourmohammadi et al. (2020), D_k, the bending stiffness of ply k is written as (see Appendix A),

$$D_k = \hat{E}_{bk} I_k + \bar{E}_k A_k l_k^2. \tag{9}$$

In Eq. (9), $\hat{E}_{bk}$ is the effective bending modulus with respect to the ply neutral axis, I_k is the second moment of area of the homogenised ply,

$$I_k = \frac{w t_k^3}{12} = \frac{w(N_k \lambda_k d_1)^3}{12}, \tag{10}$$

$\bar{E}_k$ is the tensile modulus, based on the rule of mixtures,

$$\bar{E}_k = E_{mk}\left(\pi \alpha_k^2 (\beta_k - 1) + 1\right), \tag{11}$$

A_k is the ply cross-sectional area,

$$A_k = w t_k = w N_k \lambda_k d_1, \tag{12}$$

and l_k is the lever arm of the ply (see Fig. 2),

$$l_k = \sum_{j=1}^{k} t_j - \frac{t_k}{2} = \left(\sum_{j=1}^{k} N_j \lambda_j - \frac{N_k \lambda_k}{2}\right) d_1. \tag{13}$$

In Eq. (9), $\hat{E}_{bk}$ is the effective bending modulus of ply k. In previous work (Nourmohammadi et al., 2020), we derived $\hat{E}_{bk}$ for a ply with N_k fibres, geometry ratio, α_k, and material mismatch ratio, β_k as,

$$\hat{E}_{bk} = \bar{E}_k + \frac{\pi \alpha_k^2 (3\alpha_k^2 - 1)(\beta_k - 1)}{N_k^2} E_{mk} \tag{14}$$

$$= \bar{E}_k + \frac{\pi \alpha_k^2 d_k (3\alpha_k^2 - 1)(\beta_k - 1)}{t_k^2} E_{mk}. \tag{15}$$

The bending stiffness D^{lam} of the laminate is the summation of the bending stiffness of each ply k with respect to the laminate neutral axis, D_k . For a laminate with an even number of plies,

$$D^{lam} = 2\sum_{k=1}^{P} D_k. \tag{16}$$

To calculate D_k, rather than using Eq. (9) directly, it is convenient to define the bending modulus, $\tilde{E}_{bk}$, for ply k with respect to the laminate neutral axis, using the parallel axis theorem, as:

$$\tilde{E}_{bk} = \frac{D_k}{I_k + A_k l_k^2}. \tag{17}$$

Substituting Eqs. (9) into Eq. (17) and using Eqs. (10)–(15) we obtain:

$$\tilde{E}_{bk} = \frac{\hat{E}_{bk} t_k^2 + 12\bar{E}_k \left(\sum_{j=1}^{k} t_j - \frac{t_k}{2}\right)^2}{t_k^2 + 12\left(\sum_{j=1}^{k} t_j - \frac{t_k}{2}\right)^2} \tag{18}$$

$$= \frac{\hat{E}_{bk} N_k^2 \lambda_k^2 + 12\bar{E}_k \left(\sum_{j=1}^{k} N_j \lambda_j - \frac{N_k \lambda_k}{2}\right)^2}{N_k^2 \lambda_k^2 + 12\left(\sum_{j=1}^{k} N_j \lambda_j - \frac{N_k \lambda_k}{2}\right)^2}. \tag{19}$$

For a laminate with an odd number of plies (see Appendix A), $\tilde{E}_{bk}$ is

$$\tilde{E}_{bk} = \frac{\hat{E}_{bk} t_k^2 + 12\bar{E}_k \left(\sum_{j=1}^{k} t_j - \frac{t_k + t_1}{2}\right)^2}{t_k^2 + 12\left(\sum_{j=1}^{k} t_j - \frac{t_k + t_1}{2}\right)^2} \tag{20}$$

$$= \frac{\hat{E}_{bk} N_k^2 \lambda_k^2 + 12\bar{E}_k \left(\sum_{j=1}^{k} N_j \lambda_j - \frac{N_k \lambda_k + N_1}{2}\right)^2}{N_k^2 \lambda_k^2 + 12\left(\sum_{j=1}^{k} N_j \lambda_j - \frac{N_k \lambda_k + N_1}{2}\right)^2}. \tag{21}$$

Using Eq. (16) and Eq. (17), we get

$$D^{lam} = 2\sum_{k=1}^{P} D_k = 2\sum_{k=1}^{P} \tilde{E}_{bk}(I_k + A_k l_k^2). \tag{22}$$

Finally, substituting Eq. (22) into Eq. (3), the effective bending modulus for a laminate with $2P$ plies, $\hat{E}_b^{lam}$, is

$$\hat{E}_b^{lam} = \frac{2}{t^3}\sum_{k=1}^{P}\left(t_k^3 + 12 t_k \left(\sum_{j=1}^{k} t_j - \frac{t_k}{2}\right)^2\right)\tilde{E}_{bk} \tag{23}$$

$$= \frac{\sum_{k=1}^{P}\left(N_k^3 \lambda_k^3 + 12 N_k \lambda_k \left(\sum_{j=1}^{k} N_j \lambda_j - \frac{N_k \lambda_k}{2}\right)^2\right)\tilde{E}_{bk}}{4\left(\sum_{k=1}^{P} N_k \lambda_k\right)^3}. \tag{24}$$

Similarly, the effective bending modulus for a laminate with $2P+1$ plies is:

$$\hat{E}_b^{lam} = \frac{2}{t^3}\sum_{k=2}^{P+1}\left(t_k^3 + 12 t_k \left(\sum_{j=1}^{k} t_j - \frac{t_1 + t_k}{2}\right)^2\right)\tilde{E}_{bk} + \hat{E}_{b1}\left(\frac{t_1}{t}\right)^3 \tag{25}$$

$$= \frac{2\sum_{k=2}^{P+1}\left(N_k^3 \lambda_k^3 + 12 N_k \lambda_k \left(\sum_{j=1}^{k} N_j \lambda_j - \frac{N_1 + N_k \lambda_k}{2}\right)^2\right)\tilde{E}_{bk} + \hat{E}_{b1} N_1^3}{\left(2\sum_{k=2}^{P+1} N_k \lambda_k + N_1\right)^3}. \tag{26}$$

In summary, we have used the effective bending modulus of an individual ply with respect to its neutral axis, $\hat{E}_{bk}$, and the effective tensile modulus of each ply, $\bar{E}_k$, to calculate the effective bending modulus of each ply with respect to the neutral axis of the laminate, $\tilde{E}_{bk}$. $\tilde{E}_{bk}$, is then used to calculate the bending stiffness of the laminate, D^{lam}, and thus the effective bending modulus of the laminate, $\hat{E}_b^{lam}$ is obtained. $\hat{E}_b^{lam}$ depends on the number of plies ($2P$ or $2P+1$) in the laminate, the geometry and material mismatch ratios (α_k, β_k) of the individual plies, the relative fibre spacing of each ply, λ_k, and the number of fibres in each ply, N_k.

3. Application of method: Six ply ($P = 3$) laminate of carbon and glass fibre reinforced epoxy

To illustrate the application of the method, different configurations of six-ply laminates, comprising carbon fibre-epoxy plies (c) and glass fibre-epoxy plies (g), shown in Table 1, have been considered. Typical values for the material mismatch ratio, β_c, and geometry ratio, α_c, are considered for the carbon-fibre epoxy plies:

$$\beta_c = \frac{E_{fc}}{E_m} = \frac{230\ \text{GPa}}{3\ \text{GPa}} = 76.67, \tag{27}$$

$$\alpha_c = \frac{r_c}{d_c} = \frac{5\ \mu\text{m}}{11.4\ \mu\text{m}} = 0.44, \tag{28}$$

where E_{fc} and E_m are the elastic modulus of the carbon fibre and epoxy matrix, respectively, and r_c and d_c are the fibre radius and

Table 1
Bending rigidity per unit width D^{lam}/w (N.m) for a six ply laminate with different ply thickness.

Configuration	D^{lam}/w (N.m) ($N_c = 8, N_g = 2$)	D^{lam}/w (N.m) ($N_c = 16, N_g = 4$)	*Ratio*
CCCCCC	1.175	9.41	8.01
CGCCGC	1.025	8.21	8.01
CCGGCC	1.129	9.04	8.01
CGGGGC	0.98	7.84	8.01
GCCCCG	0.61	4.89	8.01
GGCCGG	0.46	3.69	8.02
GGGGGG	0.414	3.32	8.02

fibre spacing, respectively. Similarly, a typical glass fibre epoxy ply is characterised by β_g and α_g,

$$\beta_g = \frac{E_{fg}}{E_m} = \frac{80\ \text{GPa}}{3\ \text{GPa}} = 26.67, \tag{29}$$

$$\alpha_g = \frac{r_g}{d_g} = \frac{20\ \mu\text{m}}{45.45\ \mu\text{m}} = 0.44, \tag{30}$$

where E_{fg} is the elastic modulus of the glass fibre. We consider the case when the carbon and glass fibre plies have the same thickness so $t_c = t_g$ and therefore $N_c d_c = N_g d_g$ (see Fig. 2(b)). Therefore,

$$\frac{N_c}{N_g} = \frac{d_g}{d_c} = \frac{45.45}{11.40} = 4. \tag{31}$$

Note that in Eq. (31) we have rounded to the nearest integer. To examine the effect of laminate thickness on the bending stiffness, two cases of, $N_c = 8, N_g = 2$ (Case 1) and $N_c = 16$ and $N_g = 4$ (Case 2) are considered. For Case 1, $t_c = t_g = 90.9\ \mu$m; for Case 2, $t_c = t_g = 181.8\ \mu$m, as such the number of fibres per ply and ply thickness doubles, while fibre radius and spacing remain fixed. To obtain the bending modulus of the laminate, the first step is to calculate the equivalent effective modulus, $\tilde{E}_{bk}$, for each ply. For the first ply, the effective elastic modulus, $\tilde{E}_{b1}$, is:

$$\tilde{E}_{b1} = \frac{\hat{E}_{b1} N_1^2 + 12\bar{E}_1 \left(\frac{N_1}{2}\right)^2}{N_1^2 + 12\left(\frac{N_1}{2}\right)^2} \tag{32}$$

$$= \frac{\hat{E}_{b1} + 3\bar{E}_1}{4}, \tag{33}$$

For subsequent plies,

$$\tilde{E}_{b2} = \frac{\hat{E}_{b2} N_2^2 \lambda_2^2 + 12\bar{E}_2 \left(\frac{N_2\lambda_2}{2} + N_1\right)^2}{N_2^2\lambda_2^2 + 12\left(\frac{N_2\lambda_2}{2} + N_1\right)^2}, \tag{34}$$

and

$$\tilde{E}_{b3} = \frac{\hat{E}_{b3} N_3^2 \lambda_3^2 + 12\bar{E}_3 \left(\frac{N_3\lambda_3}{2} + N_2\lambda_2 + N_1\right)^2}{N_3^2\lambda_3^2 + 12\left(\frac{N_3\lambda_3}{2} + N_2\lambda_2 + N_1\right)^2}. \tag{35}$$

The bending stiffness per unit width of the laminate, D^{lam}/w, is then,

$$\frac{D^{lam}}{w} = \frac{t^3}{6}\left(4\tilde{E}_{b1} + 13\tilde{E}_{b2} + 49\tilde{E}_{b3}\right). \tag{36}$$

D^{lam}/w for different configurations of glass and carbon fibre plies can be calculated from Eq. (36) and the results for both cases are shown in Table 1. The results show that, as expected, the highest bending stiffness per unit width is for the all carbon laminate and the lowest stiffness is the all glass laminate with other combinations falling in between. It may also be noted that the thicker laminate, as expected for a larger laminate, has the higher bending stiffness. In the first case, a laminate with plies of thickness t and in the second case, plies of $2t$ are studied (i.e. the numbers of fibres are doubled for case 2). For a homogeneous ply (not heterogeneous material) of thickness t, then by increasing the ply thickness to $2t$, the second moment of area ($I = bt^3/12$) for the second case is eight times that of the first case. However, for the cases examined in Table 1, the ratio of bending stiffness is not a fixed value (8), due to the size effect in the calculation of $\tilde{E}_{bk}$. In other words, there is a size effect by scaling the thickness of plies, though the effect is small for this particular example. This example shows a somewhat minor size effect due to ply scaling which is most pronounced in the hybrid laminate (approximately 0.25%).

4. Comparison with results of Wheel et al. (2015)

4.1. Comparison of effective bending modulus

As discussed in Section 2, Wheel et al. (2015) did not examine underlying ply microstructure and used the tensile modulus from the rule of mixtures, $\bar{E}_k$, to represent the homogenised ply bending modulus. For a laminate of the type shown in Fig. 2 with $2P$ plies, the effective laminate bending modulus consistent with the Wheel et al. (2015) approach, here designated $\breve{E}_b^{lam}$, is obtained by replacing $\tilde{E}_{bk}$ in Eqs. (23) and (24), by $\bar{E}_k$ to obtain,

$$\breve{E}_b^{lam} = \frac{2}{t^3}\sum_{k=1}^{P}\left(t_k^3 + 12t_k\left(\sum_{j=1}^{k} t_j - \frac{t_k}{2}\right)^2\right)\bar{E}_k \tag{37}$$

$$= \frac{\sum_{k=1}^{P}\left(N_k^3\lambda_k^3 + 12N_k\lambda_k\left(\sum_{j=1}^{k} N_j\lambda_j - \frac{N_k\lambda_k}{2}\right)^2\right)\bar{E}_k}{4\left(\sum_{k=1}^{P} N_k\lambda_k\right)^3}. \tag{38}$$

Similarly for a laminate with $2P+1$ plies,

$$\breve{E}_b^{lam} = \frac{2}{t^3}\sum_{k=2}^{P+1}\left(t_k^3 + 12t_k\left(-\frac{t_1 + t_k}{2} + \sum_{j=1}^{k} t_j\right)^2\right)\bar{E}_k + \bar{E}_1\left(\frac{t_1}{t}\right)^3 \tag{39}$$

$$= \frac{2\sum_{k=2}^{P+1}\left(N_k^3\lambda_k^3 + 12N_k\lambda_k\left(-\frac{N_1 + N_k\lambda_k}{2} + \sum_{j=1}^{k} N_j\lambda_j\right)^2\right)\bar{E}_k + \bar{E}_1 N_1^3}{\left(2\sum_{k=2}^{P+1} N_k\lambda_k + N_1\right)^3}. \tag{40}$$

In order to quantify the difference between the two approaches, a relative modulus variation, R, is defined as:

$$R = \frac{\hat{E}_b^{lam} - \breve{E}_b^{lam}}{\breve{E}_b^{lam}}. \tag{41}$$

The difference between the effective moduli $\hat{E}_b^{lam}$ and $\breve{E}_b^{lam}$ is due to the dependency of $\hat{E}_b^{lam}$ on the number of fibres in each ply while $\breve{E}_b^{lam}$ depends only on ply thickness. This is due to the fact that $\hat{E}_b^{lam}$ in Eqs. (23) and (24) depends on $\tilde{E}_{bk}$ (which depends on $\hat{E}_{bk}$) while $\breve{E}_b^{lam}$ in Eqs. (37) and (38) depends only on $\bar{E}_k$. Thus $\tilde{E}_{bk}$ has an additional dependence on the number of fibres in each ply, while $\bar{E}_k$ in Eq. (11) depends only on ply thickness. In other words, laminates with the same number of plies and the same ply thickness, but with different numbers of fibres in each ply, can have a different bending modulus, $\hat{E}_b^{lam}$. Thus, R, defined in Eq. (41) quantifies the effect of microstructure at the ply level (number of fibres) not captured by the Wheel et al. (2015) approach.

In order to show the difference between the two approaches, two simple examples of a three ply ($P = 1$) laminate, illustrated in Fig. 3, have been considered. The plies have the same number of fibres, $N_1 = N_2 = N$, the same geometry ratio, $\alpha_1 = \alpha_2 = \alpha$, and the same material mismatch ratio, $\beta_1 = \beta_2 = \beta$, but different fibre spacing, $\lambda_2 \neq 1$. In Fig. 3, $\alpha = 0.48$ and four cases of $\beta = 0, 0.2, 2$ and 20 have been considered. The dependence of R on N, for different values of λ_2, is shown. Fig. 3(a) and (b) show that for $\beta < 1, R$ is positive and as β increases (approaches 1), the magnitude of R decreases. From Fig. 3(c) and (d) it is noted that for $\beta > 1, R$ is negative and as β increases, the magnitude of R increases. Fig. 3 shows that for some ply configurations, $|R| > 5\%$, indicating that the ply microstructure significantly affects the bending stiffness of the laminate.

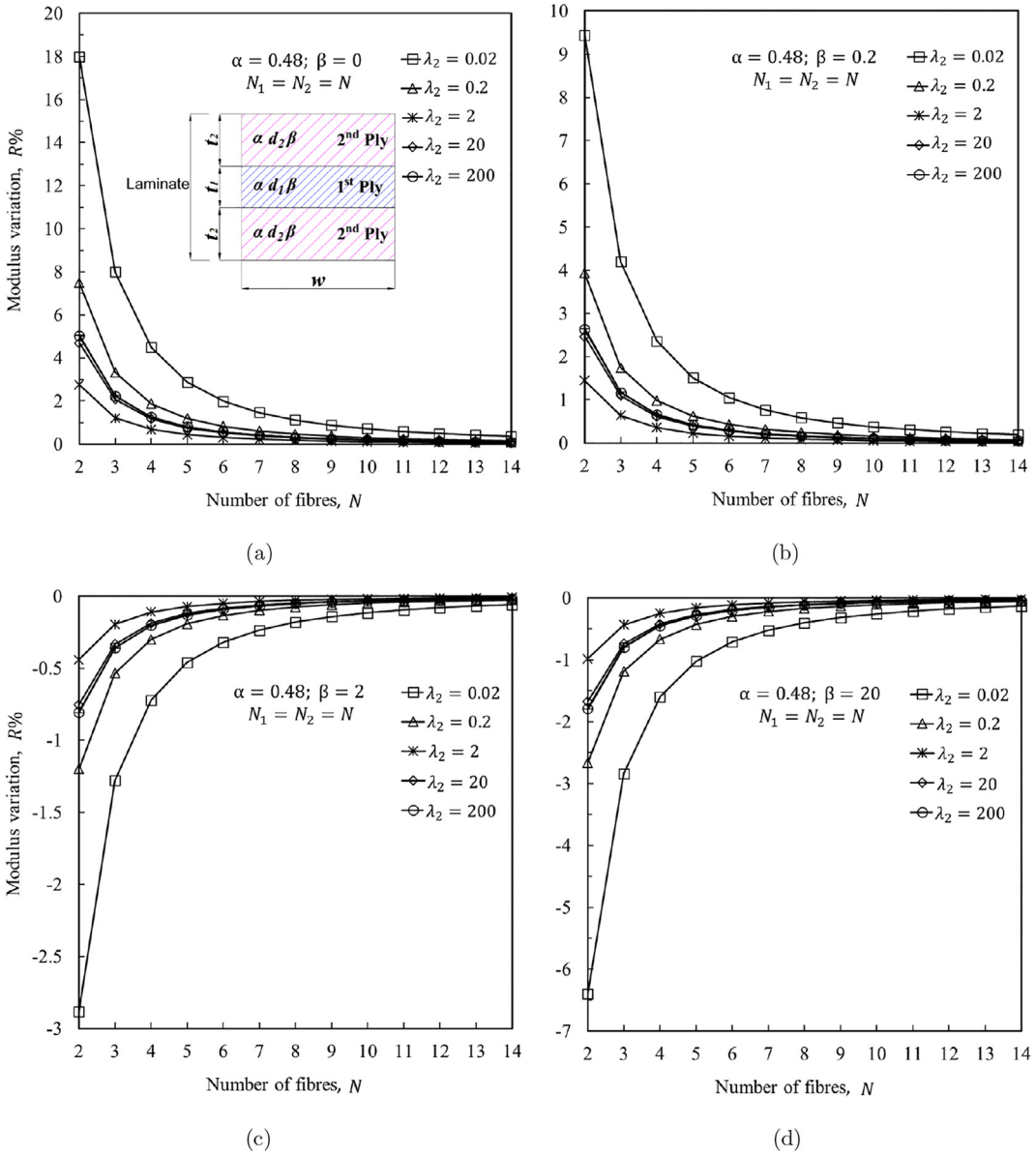

Fig. 3. Modulus variation R for three-ply laminate for constant geometry ratio of $\alpha = 0.48$ as function of material mismatch ratio of β and number of fibres N in a ply for different values of λ_2; (a) For $\beta = 0$; (b) For $\beta = 0.2$; (c) For $\beta = 2$; (d) For $\beta = 20$.

4.2. Effect of fibre spacing ratio, λ_2, on modulus variation, R

Fig. 4 considers a three-ply laminate, where the thickness of the second ply, t_2, is varied. Again $\alpha_1 = \alpha_2 = \alpha = 0.48$. In this case we consider $\beta_1 = 50$ (very stiff fibres) and $\beta_2 = 0$ (no reinforcement) and the fibre spacing in the first ply, $d_1/t_1 = 0.5$. Two cases of fibre spacing ratio, $\lambda_2 = 0.1$ and 10 are considered. By selecting a fixed value of t_2/t_1 in Fig. 4, the ply thickness, t_2, and volume fraction ratio, v_f, remain constant (as t_1 and α are constants). Each curve has a different value of λ, which is related to fibre spacing, d, and identical value of α ($\alpha = r/d$), resulting in each curve having a different r value. As thickness ($t = Nd$) is constant and d is different for both curves, they have different values of N. Thus for a fixed value of t_2/t_1, while v_f is the same for both curves, N, d and r are different for each curve. As a result, for a fixed value of t_2/t_1 on each curve, while $\breve{E}_b^{lam}$ is identical (from Eq. (40)), they have different $\hat{E}_b^{lam}$ values (from Eq. (25)) which cause to have different R values.

The size effect is related to either ply thickness or internal ply microstructure. In each curve of Fig. 4, the effect of normalised thickness, t_2/t_1, on modulus variation, R, can be investigated. A large R means a large size effect. We can consider t_1 as fixed and then increasing t_2/t_1 means increasing the thickness of ply 2. As shown by increasing $t_2/t_1, R$ decreases and reaches zero, i.e. the size effect disappears. By comparing the value of R for a fixed value of thickness, t_2/t_1, (the same thickness for t_2, if t_1 is fixed.) the influence of internal ply microstructure on the size effect can be explored. As shown in Fig. 4, R is higher for $\lambda_2 = 10$ compared to $\lambda_2 = 0.1$ for the same thickness. Thus increasing fibre spacing, while keeping the ply thickness constant, leads to a size effect. However, from Eq. (26), two different values for effective bending modulus, $\hat{E}_b^{lam}$, are obtained. It may be noted for the case $\lambda = 0.1, R \approx 0$, which implies that, in this case, the effective bending modulus of the laminate is closely approximated by $\breve{E}_b^{lam}$, through Eq. (40), while for $\lambda_2 = 10, R > 4\%$ when $t_2/t_1 < 10$.

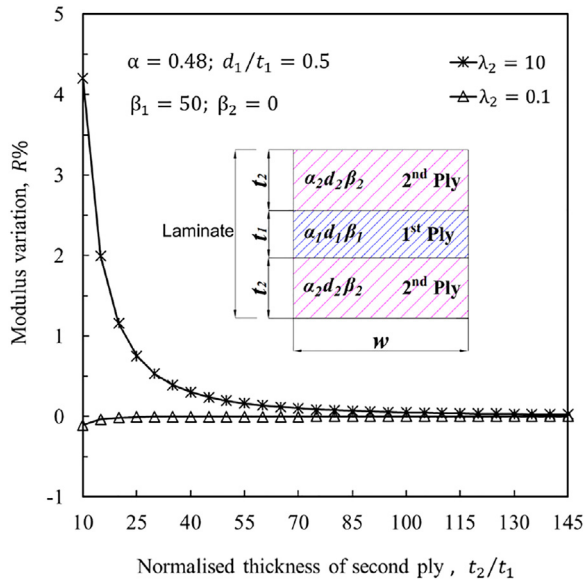

Fig. 4. Modulus variation R% for different second ply thickness t_2 in a three-ply laminate.

4.3. Difference in nature of size effect for a laminate

In Wheel et al. (2015) Wheel et al. showed that the nature of the size effect depends on the stiffness of the outer ply of a laminated beam. In their study a laminate is considered to comprise multiple repeating units of a three-ply 'sub-laminate'. As the number of repeating units increases, the bending modulus, $\breve{E}_b^{lam}$, approaches the effective tensile modulus calculated by the rule of mixtures, $\bar{E}^{lam}$. For a laminate with $2P+1$ plies:

$$\bar{E}^{lam} = \frac{2}{t}\sum_{k=2}^{P+1}\bar{E}_k t_k + \bar{E}_1\frac{t_1}{t}. \tag{42}$$

For a three-ply laminate ($P=1$), if $\bar{E}_2 > \bar{E}_1$ it is straightforward to show that $\breve{E}_b^{lam}$ is greater than $\bar{E}^{lam}$, which means that the rule of mixtures underestimates the effective bending modulus, $\breve{E}_b^{lam}$. This implies a positive size effect, since by increasing the number of sub-laminates the value of $\breve{E}_b^{lam}$ decreases and approaches $\bar{E}^{lam}$. Similarly, if $\bar{E}_2 < \bar{E}_1$ then $\breve{E}_b^{lam} < \bar{E}^{lam}$, resulting in a negative size effect.

Accounting for the microstructure at the ply level can cause the nature of the size effect to be different from that predicted by Wheel et al. (2015). In Tables 2 and 3, we consider two cases. Following the approach of Wheel et al. (2015), Case 1 predicts a positive size effect, since $\bar{E}_2 > \bar{E}_1$ and $\breve{E}_b^{lam} > \bar{E}^{lam}$. Case 2 predicts no size effect since $\bar{E}_2 = \bar{E}_1$ and $\breve{E}_b^{lam} = \bar{E}^{lam}$. However, for the particular microstructures chosen in Table 2, both cases demonstrate a negative size effect, since $\hat{E}_b^{lam} < \bar{E}^{lam}$ for both cases. This demonstrates that the microstructure at the ply level, can influence the nature as well as the magnitude of the size effect of the laminate as confirmed by the result shown in Table 2. The terms $Err_1 = (\breve{E}_b^{lam} - \bar{E}^{lam})/\bar{E}^{lam}$ and $Err_2 = (\hat{E}_b^{lam} - \bar{E}^{lam})/\bar{E}^{lam}$ are introduced to evaluate the relative difference of $\hat{E}_b^{lam}$ and $\bar{E}^{lam}$. As shown, the absolute value of error is higher for the case of Err_2 due to consideration of internal ply microstructure. By increasing the number of plies for both cases the bending modulus, $\hat{E}_b^{lam}$ approaches $\bar{E}^{lam}$, demonstrating a negative size effect.

5. Equivalent composite laminate model for a generalized continuum

As discussed previously (Nourmohammadi et al., 2020), the size-dependent behaviour of a composite ply under bending can be represented using a generalised continuum approach (micropolar theory), in which the bending modulus is represented by two terms, one independent of size and a second, size dependent term, with an associated characteristic length. Based on the results presented here, by rewriting Eqs. (23)–(26), the bending modulus of a multi-ply laminate, $\hat{E}_b^{lam}$, can be represented as,

$$\hat{E}_b^{lam} = \bar{E}^{lam}\left(1 + \left(\frac{\hat{l}}{t}\right)^2\right), \tag{43}$$

with

$$\frac{\hat{l}}{t} = \sqrt{\frac{\hat{E}_b^{lam}}{\bar{E}^{lam}} - 1}. \tag{44}$$

Previously (Nourmohammadi et al., 2020), we showed that for a single ply with N fibres, geometry ratio, α and material mismatch ratio, β, then

$$\frac{\hat{l}}{t} = \frac{1}{N}\sqrt{\frac{\pi\alpha^2(3\alpha^2-1)(\beta-1)}{\pi\alpha^2(\beta-1)+1}}. \tag{45}$$

Due to the complexity of the expression for $\hat{E}_b^{lam}$ it is not possible to provide a general closed form expression for $\hat{l}$ representing an arbitrary laminate. As an example, consider a three-ply laminate as shown in Fig. 5. Here, the normalised characteristic length, $\hat{l}/t$, as a function of N_1 and N_2 is depicted. We have already showed (Nourmohammadi et al., 2020) that for a singe ply $\hat{l}/t$ increases as N decreases (see Eq. (45)). However,for a multi-ply laminate, having thinner plies in a laminate does not necessarily mean that $\hat{l}/t$ increases. For example, in Fig. 5, when $N_1 = 2$ as N_2 decreases (ply thickness decreases) $\hat{l}/t$ also decreases. Conversely, for $N_2 = 2$, as N_1 decreases $\hat{l}/t$ increases. Thus the nature of the size effect, as quantified by $\hat{l}$, depends on the ply microstructure.

According to Eq. (44), a characteristic length, $\hat{l}$ can be defined only if the ratio $\hat{E}_b^{lam}/\bar{E}^{lam} > 1$. For a single-ply laminate, this implies, using Eq. (45), that $\hat{l}$ can be defined only for $\beta > 1$. For the case of a multi-ply laminate the condition $\hat{E}_b^{lam}/\bar{E}^{lam} > 1$ cannot be easily simplified. As an example, for the case illustrated in Fig. 5 ($P=1, N_1=2, N_2=2, \alpha_1=\alpha_2=0.1, \beta_1=0.01, \beta_2=100$), $\hat{l}$ only exists if $\lambda_2 < 9$.

Table 2
Size effect in the laminate due to ply microstructure for $N_1 = N_2 = 2$.

case	α_1	β_1	α_2	β_2	λ_2	E_m MPa	$\bar{E}_1$ MPa	$\bar{E}_2$ MPa	$\breve{E}_b^{lam}$ MPa	$\hat{E}_b^{lam}$ MPa	$\bar{E}^{lam}$ MPa	Err_1 %	Err_2 %
1	0.2	155	0.2	170	0.01	25	508.8	555.9	511.5	411.2	509.7	0.3	-19.3
2	0.3	25	0.2	55	0.01	25	194.6	194.6	194.6	165.5	194.6	0	-15

Table 3
Effect of increasing number of plies on the laminate examined in Table 2.

case	number of plies	$\hat{E}_b^{lam}$	$\bar{E}^{lam}$	$Err\%$
1	3	411.2	509.7	−19.3
1	7	498.5	509.4	−2.1
1	11	505.5	509.3	−0.8
1	15	507.4	509.7	−0.4
2	3	165.5	194.6	15.0
2	7	191.3	194.6	1.7
2	11	193.4	194.6	0.6
2	15	194.0	194.6	0.3

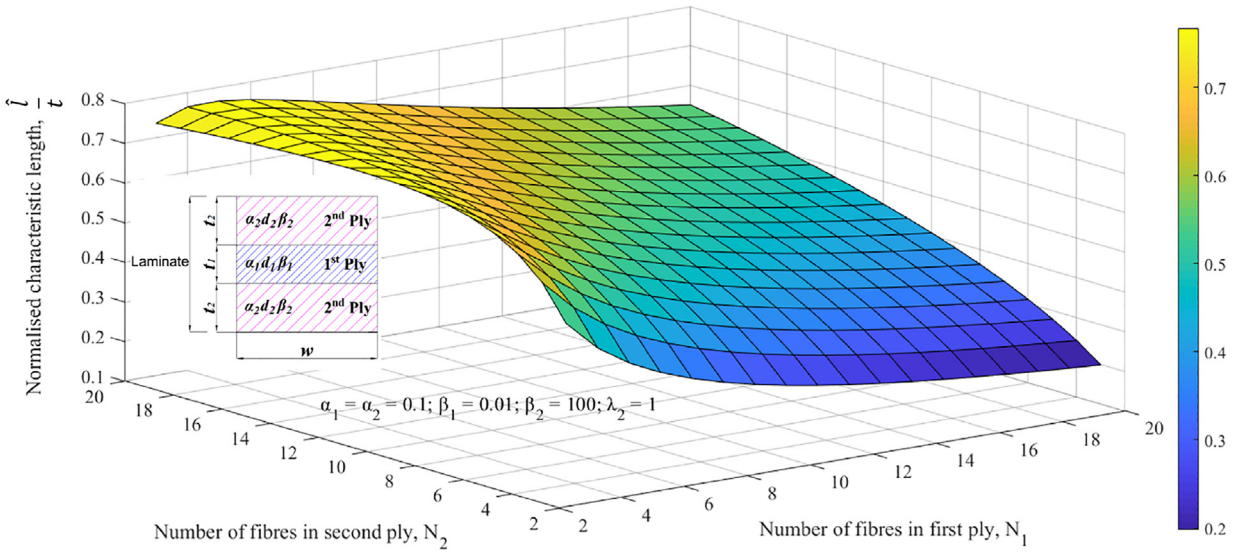

Fig. 5. Normalised characteristic length for a symmetric three-ply laminate.

6. Conclusions

In this work, the effective bending modulus of a fibre composite laminate comprising unidirectional plies has been calculated. The results show that the bending modulus of the laminate depends on the number of plies, the number of fibres in each ply, the ply geometry ratio, the ply material mismatch ratio, and the fibre spacing ratio.

The results have been compared with those in Wheel et al. (2015), which does not consider ply microstructure, but instead considers each ply as being homogenous. In some cases significant differences have been identified between the two approaches. As an example, for a three-ply laminate with two fibres through the thickness of each ply, the bending stiffness can differ by 10%. Indeed the opposite trend with respect to laminate size has been identified for certain combinations of ply properties (i.e. effective bending modulus is predicted to decrease with increasing size in Wheel et al. (2015) while it increases with increasing size using the current approach).

The bending behaviour of a heterogeneous composite ply has been modelled in Cauchy media in which there is just translational degrees of freedom and the stress tensor is proportional to the strain tensor. As analysing a heterogeneous model is computationally expensive, an equivalent homogenised model using a generalised continuum has been introduced. For this purpose, micropolar theory has been used in which there are independent rotational degrees of freedom in addition to translational ones. Furthermore, there are micro-moments in addition to forces to equilibrate the non-symmetrical part of shear stress. In micropolar theory, the bending characteristic length, $\hat{l}$, for a multi-ply laminate has been provided which can be used to calculate the new material constituents.

The effect of inter-ply microstructure on the bending behaviour of a composite laminate is considered in our future work. For this purpose, the fibres are shifted from their regular position by ε in a symmetric cross-section. Fibre arrangement in a composite ply will affect its bending behaviour as the position of fibres will affect the second moment of the area used in the Euler-Bernoulli beam model.

Declaration of Competing Interest

The authors declare that they have no known competing financial interests or personal relationships that could have appeared to influence the work reported in this paper.

Acknowledgments

NN and PMW would like to acknowledge funding from Science Foundation Ireland (SFI) and Temporally VARIable COMPosite (VARICOMP) Grant No. (15/RP/2773) under its Research Professorship programme.

Appendix A. Derivation of effective bending modulus of a laminate

This Appendix describes in more detail the method to determine the effective bending modulus of a laminate, which is sum-

marised in the main text. In Fig. A.1 a material region within a ply k is defined as the region containing a single fibre of radius r with its surrounding matrix. The area of the material region is $d \times d$ where d is the fibre spacing in the ply. The c-axis in Fig. A.1 is the neutral axis of the material region; the a-axis, is the neutral axis of the ply and the b-axis is the neutral axis of the laminate. The distance l in Fig. A.1 is the distance from the a axis of ply k to the b-axis of the laminate. The distance s_i is the distance of the c axis for material region i from the a axis for the ply. For a ply with an even number of fibres,

$$s_i = (2i-1)d/2, \tag{A.1}$$

with $i = 1$ corresponding to the material region closest to the a axis and $i = N/2$ corresponding to the material region furthest from the a axis. For a ply with an odd number of fibres,

$$s_i = (i-1)d, \tag{A.2}$$

with $i = 1$ corresponding to the material region closest to the a axis and $i = (N+1)/2$ corresponding to the material region furthest from the a axis.

A.1. Analysis for a single ply

To determine the total bending stiffness of the laminate, we first determine the bending stiffness for a ply with respect to the neutral axis of the laminate (the b axis) by considering the stiffness contribution of each material region within the ply. The bending stiffness, $\hat{D}$, of a single ply with respect to the ply neutral axis (the a-axis) is given by

$$\hat{D} = \sum_{i=1}^{N} E_m I^i_{a|m} + E_f I^i_{a|f}, \tag{A.3}$$

where E_m and E_f are the matrix and fibre modulus, respectively, $I^i_{a|m}$ and $I^i_{a|f}$ are the second moment of area about the a-axis for the matrix and the fibre regions, respectively, within material region i. For the case of N even number of fibres in a ply by symmetry,

$$\hat{D} = 2\sum_{i=1}^{\frac{N}{2}} \left(E_m I^i_{a|m} + E_f I^i_{a|f} \right). \tag{A.4}$$

Using the parallel axis theorem and considering Eq. (A.1), $I^i_{a|m}$ and $I^i_{a|f}$ are given by

$$I^i_{a|m} = I_{c|m} + A_m s_i^2 = I_{c|m} + A_m \left(\frac{2i-1}{2}\right)^2 d^2, \tag{A.5}$$

$$I^i_{a|f} = I_{c|f} + A_f s_i^2 = I_{c|f} + A_f \left(\frac{2i-1}{2}\right)^2 d^2, \tag{A.6}$$

where $I_{c|m}$ and $I_{c|f}$ are the second moment of area for the matrix and fibre regions, respectively, with respect to the neutral axis of each material region (the c-axis) and A_m and A_f are the matrix and fibre areas, respectively. Note that $I_{c|m}, I_{c|f}, A_m$ and A_f are independent of the position of region i within the ply. For simplicity of notation we do not include the subscript k in these equations, e.g d in Eq. (A.5) refers to the spacing d_k for a particular ply k, illustrated in Fig. A.1.

The bending stiffness of the ply with respect to the laminate neutral axis (b-axis) is given by

$$D = \sum_{i=1}^{N} E_m I^i_{b|m} + E_f I^i_{b|f}, \tag{A.7}$$

where $I^i_{b|m}$ and $I^i_{b|f}$ are the second moment of area about the b-axis for the matrix and the fibre regions, respectively, within material region i. For material regions above the a-axis, the second moment of area, $I^i_{b|m}$ and $I^i_{b|f}$ for the matrix and fibre, with respect to the b-axis, again using the parallel axis theorem are:

$$I^i_{b|m} = I_{c|m} + A_m \left[\left(\frac{2i-1}{2}\right) d + l \right]^2 \tag{A.8}$$

$$= I_{c|m} + A_m \left[\left(\frac{2i-1}{2}\right)^2 d^2 + l^2 + (2i-1)dl \right], \tag{A.9}$$

$$I^i_{b|f} = I_{c|f} + A_f \left[\left(\frac{2i-1}{2}\right) d + l \right]^2 \tag{A.10}$$

$$= I_{c|f} + A_f \left[\left(\frac{2i-1}{2}\right)^2 d^2 + l^2 + (2i-1)dl \right]. \tag{A.11}$$

By substituting Eq. (A.5) into (A.9) and Eq. (A.6) into (A.11), we have:

$$I^i_{b|m} = I^i_{a|m} + A_m \left[l^2 + (2i-1)dl \right], \tag{A.12}$$

$$I^i_{b|f} = I^i_{a|f} + A_f \left[l^2 + (2i-1)dl \right]. \tag{A.13}$$

For material regions below the a-axis, the second moment of area, $I^i_{b|m}$ and $I^i_{b|f}$ for matrix and fibre regions are:

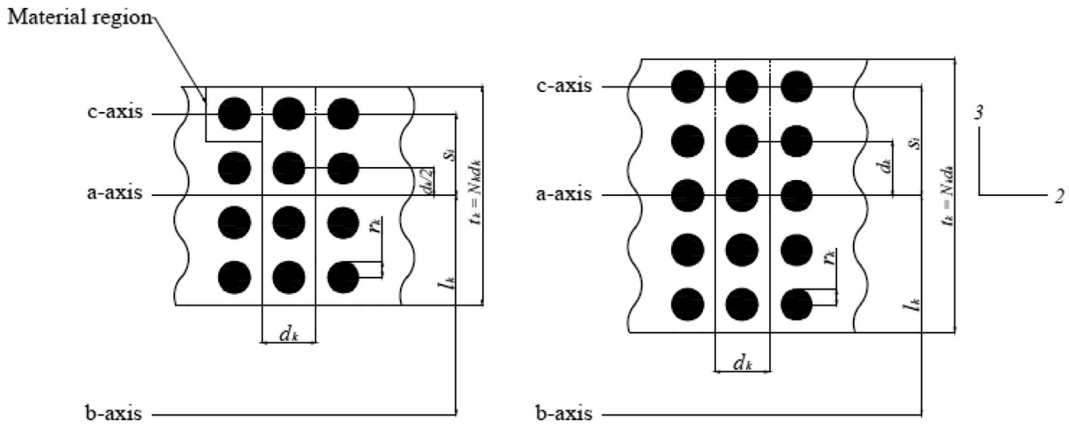

Fig. A.1. Configuration of fibres in a composite ply with even (left) and odd (right) number of fibres.

$$I^i_{b|m} = I_{c|m} + A_m\left[\left(\frac{2i-1}{2}\right)d - l\right]^2 \tag{A.14}$$

$$= I_{c|m} + A_m\left[\left(\frac{2i-1}{2}\right)^2 d^2 + l^2 - (2i-1)dl\right], \tag{A.15}$$

$$I^i_{b|f} = I_{c|f} + A_f\left[\left(\frac{2i-1}{2}\right)d - l\right]^2 \tag{A.16}$$

$$= I_{c|f} + A_f\left[\left(\frac{2i-1}{2}\right)^2 d^2 + l^2 - (2i-1)dl\right]. \tag{A.17}$$

By substituting Eq. (A.5) into (A.15) and Eq. (A.6) into (A.17), we have:

$$I^i_{b|m} = I^i_{a|m} + A_m\left[l^2 - (2i-1)dl\right], \tag{A.18}$$

$$I^i_{b|f} = I^i_{a|f} + A_f\left[l^2 - (2i-1)dl\right]. \tag{A.19}$$

Then from Eq. (A.7), we have:

$$D = \sum_{i=1}^{\frac{N}{2}} E_m\left(I^i_{a|m} + A_m\left[l^2 + (2i-1)dl\right]\right) + E_m\left(I^i_{a|m} + A_m\left[l^2 - (2i-1)dl\right]\right) + \sum_{i=1}^{\frac{N}{2}} E_f\left(I^i_{a|f} + A_f\left[l^2 + (2i-1)dl\right]\right) + E_f\left(I^i_{a|f} + A_f\left[l^2 - (2i-1)dl\right]\right) \tag{A.20}$$

$$= 2\sum_{i=1}^{\frac{N}{2}} E_m\left(I^i_{a|m} + A_m l^2\right) + 2\sum_{i=1}^{\frac{N}{2}} E_f\left(I^i_{a|f} + A_f l^2\right) \tag{A.21}$$

$$= 2\sum_{i=1}^{\frac{N}{2}} (E_m I^i_{a|m} + E_f I^i_{a|f}) + N(E_m A_m + E_f A_f) l^2. \tag{A.22}$$

We rewrite Eq. (A.22) in terms of $\bar{E}$, the effective tensile modulus of the ply calculated by the rule of mixtures,

$$\bar{E} = \frac{E_m A_m + E_f A_f}{A_m + A_f}, \tag{A.23}$$

$$\Rightarrow N(E_m A_m + E_f A_f) = \bar{E}A, \tag{A.24}$$

where A is the total area of the ply. Substituting Eq. (A.24) in Eq. (A.22) we get,

$$D = 2\sum_{i=1}^{\frac{N}{2}} \left(E_m I^i_{a|m} + E_f I^i_{a|f}\right) + \bar{E}Al^2. \tag{A.25}$$

Using Eq. (A.4) we write,

$$D = \hat{D} + \bar{E}Al^2. \tag{A.26}$$

For N an odd number of fibres in a ply, illustrated in Fig. A.1, a corresponding approach is followed. The bending rigidity, $\hat{D}$ for a ply with respect to the ply neutral axis, a-axis, is:

$$\hat{D} = 2\sum_{i=2}^{\frac{N+1}{2}} \left(E_m I^i_{a|m} + E_f I^i_{a|f}\right) + (E_m I_{c|m} + E_f I_{c|f}). \tag{A.27}$$

The second moment of area of material region i about the a-axis is given by

$$I^i_{a|m} = I_{c|m} + A_m s_i^2 = I_{c|m} + A_m(i-1)^2 d^2, \tag{A.28}$$

$$I^i_{a|f} = I_{c|f} + A_f s_i^2 = I_{c|f} + A_f(i-1)^2 d^2. \tag{A.29}$$

For a material region i above the a-axis, the second moment of area, $I^i_{b|m}$ and $I^i_{b|f}$ for matrix and fibre regions are:

$$I^i_{b|m} = I_{c|m} + A_m[(i-1)d + l]^2 \tag{A.30}$$

$$= I_{c|m} + A_m\left[(i-1)^2 d^2 + l^2 + 2(i-1)dl\right], \tag{A.31}$$

$$I^i_{b|f} = I_{c|f} + A_f[(i-1)d + l]^2 \tag{A.32}$$

$$= I_{c|f} + A_f\left[(i-1)^2 d^2 + l^2 + 2(i-1)dl\right]. \tag{A.33}$$

Substituting Eq. (A.28) in A.31 and Eq. (A.29) in A.33, we have:

$$I^i_{b|m} = I^i_{a|m} + A_m\left[l^2 + 2(i-1)dl\right], \tag{A.34}$$

$$I^i_{b|f} = I^i_{a|f} + A_f\left[l^2 + 2(i-1)dl\right]. \tag{A.35}$$

For a material region i below the a-axis, the second moments of area, $I^i_{b|m}$ and $I^i_{b|f}$, for matrix and fibre regions are:

$$I^i_{b|m} = I_{c|m} + A_m[(i-1)d - l]^2 \tag{A.36}$$

$$= I_{c|m} + A_m\left[(i-1)^2 d^2 + l^2 - 2(i-1)dl\right]. \tag{A.37}$$

$$I^i_{b|f} = I_{c|f} + A_f[(i-1)d - l]^2 \tag{A.38}$$

$$= I_{c|f} + A_f\left[(i-1)^2 d^2 + l^2 - 2(i-1)dl\right]. \tag{A.39}$$

By substituting Eq. (A.28) in (A.37) and Eq. (A.29) in (A.39), we have:

$$I^i_{b|m} = I^i_{a|m} + A_m\left[l^2 - 2(i-1)dl\right], \tag{A.40}$$

$$I^i_{b|f} = I^i_{a|f} + A_f\left[l^2 - 2(i-1)dl\right]. \tag{A.41}$$

and for the central region (the region containing the a-axis in Fig. A.1), designated as region 1:

$$I^1_{b|m} = I^1_{a|m} + A_m l^2 = I_{c|m} + A_m l^2, \tag{A.42}$$

$$I^1_{b|f} = I^1_{a|f} + A_f l^2 = I_{c|f} + A_f l^2. \tag{A.43}$$

Then, from Eq. (A.7), we have:

$$D = \sum_{i=2}^{\frac{N+1}{2}} E_m\left(I^i_{a|m} + A_m\left[l^2 + (2i-1)dl\right]\right) + E_m\left(I^i_{a|m} + A_m\left[l^2 - (2i-1)dl\right]\right) + \sum_{i=2}^{\frac{N+1}{2}} E_f\left(I^i_{a|f} + A_f\left[l^2 + (2i-1)dl\right]\right) + E_f\left(I^i_{a|f} + A_f\left[l^2 - (2i-1)dl\right]\right) + E_m(I_{c|m} + A_m l^2) + E_f(I_{c|f} + A_f l^2) \tag{A.44}$$

$$= 2\sum_{i=2}^{\frac{N+1}{2}} E_m\left(I^i_{a|m} + A_m l^2\right) + 2\sum_{i=2}^{\frac{N+1}{2}} E_f\left(I^i_{a|f} + A_f l^2\right) + E_m(I_{c|m} + A_m l^2) + E_f(I_{c|f} + A_f l^2) \tag{A.45}$$

$$= E_m I_{c|m} + E_f I_{c|f} + 2\sum_{i=2}^{\frac{N+1}{2}} (E_m I^i_{a|m} + E_f I^i_{a|f}) + N(E_m A_m + E_f A_f) l^2. \tag{A.46}$$

By substituting Eq. (A.24) in Eq. (A.46) we get:

$$D = E_m I_{c|m} + E_f I_{c|f} + 2\sum_{i=2}^{\frac{N+1}{2}} \left(E_m I^i_{a|m} + E_f I^i_{a|f}\right) + \bar{E}Al^2, \tag{A.47}$$

Using Eq. (A.27) we write,

$$D = \hat{D} + \bar{E}Al^2. \tag{A.48}$$

It may be seen that the expression for D, the bending stiffness of the ply about the laminate neutral axis is the same for an odd and even number of fibres.

For both cases, we write $\hat{D}$ in terms of the bending modulus of the ply with respect to the ply neutral axis, $\hat{E}_b$, and the homogenised second moment of area of the ply, I,

$$\hat{D} = \hat{E}_b I, \tag{A.49}$$

where

$$I = \frac{wt^3}{12} = \frac{w(Nd)^3}{12}, \tag{A.50}$$

where w is the overall width of the ply. Then,

$$D = \hat{E}_b I + \bar{E} A l^2. \tag{A.51}$$

The effective bending modulus $\tilde{E}_b$ of the ply with respect to the neutral axis of the laminate (the b-axis) is defined as

$$\tilde{E}_b = \frac{D}{I + Al^2} \tag{A.52}$$

$$= \frac{\hat{E}_b I + \bar{E} A l^2}{I + Al^2} \tag{A.53}$$

$$= \frac{\hat{E}_b N^2 d^2 + 12\bar{E} l^2}{N^2 d^2 + 12 l^2}. \tag{A.54}$$

A.2. Summing over multiple plies

In this section, the index k is re-introduced to represent ply k within the multi-ply laminate. We calculate the effective bending modulus of the laminate, $\hat{E}_b^{lam}$, for an even number of plies, $2P$. The analysis is similar for an odd number of plies and is omitted in the interests of space. The lever arm l_k for ply k with respect to the laminate neutral axis, the b-axis, is:

$$l_k = -\frac{t_k}{2} + \sum_{j=1}^{k} t_j, \tag{A.55}$$

where t_k is the ply thickness and $k = 1$ corresponds to the ply closest to the laminate neutral axis and $k = P$ corresponds to the ply furthest from the neutral axis. As in the main text, the fibre spacing ratio is defined,

$$\lambda_k = d_k / d_1, \tag{A.56}$$

and then, from Fig. A.1,

$$t_k = N_k \lambda_k d_1. \tag{A.57}$$

By substituting Eq. (A.57) into Eq. (A.55), we have:

$$l_k = \left(-\frac{N_k \lambda_k}{2} + \sum_{j=1}^{k} N_j \lambda_j \right) d_1. \tag{A.58}$$

Writing Eq. (A.54) for each ply k and substituting for l_k from Eq. (A.58),

$$\tilde{E}_{bk} = \frac{\hat{E}_{bk} N_k^2 \lambda_k^2 + 12\bar{E}_k \left(-\frac{N_k \lambda_k}{2} + \sum_{j=1}^{k} N_j \lambda_j \right)^2}{N_k^2 \lambda_k^2 + 12 \left(-\frac{N_k \lambda_k}{2} + \sum_{j=1}^{k} N_j \lambda_j \right)^2}. \tag{A.59}$$

We define the effective bending modulus of the laminate, $\hat{E}_b^{lam}$, as:

$$\hat{E}_b^{lam} = \frac{D^{lam}}{I^{lam}}, \tag{A.60}$$

where D^{lam} is the bending stiffness of the laminate and I^{lam} is the second moment of the homogenised laminate,

$$I^{lam} = \frac{wt^3}{12}, \tag{A.61}$$

where t is the laminate thickness,

$$t = 2\sum_{k=1}^{P} t_k. \tag{A.62}$$

Finally, to obtain D^{lam}, we sum over the bending stiffness of the individual plies, D_k, in the laminate,

$$D^{lam} = 2\sum_{k=1}^{P} D_k = 2\sum_{k=1}^{P} \tilde{E}_{bk} (I_k + A_k l_k^2). \tag{A.63}$$

The bending modulus of the laminate, $\hat{E}_b^{lam}$, is then

$$\hat{E}_b^{lam} = \frac{2\sum_{k=1}^{P} \tilde{E}_{bk} (I_k + A_k l_k^2)}{I} \tag{A.64}$$

$$= \frac{2\sum_{k=1}^{P} (t_k^3 + 12 t_k l_k^2) \tilde{E}_{bk}}{t^3}. \tag{A.65}$$

By substituting Eq. (A.57) in Eq. (A.65), we can write in terms of the number of fibres in each ply, N_k,

$$\hat{E}_b^{lam} = \frac{2\sum_{k=1}^{P} \left(N_k^3 \lambda_k^3 + 12 N_k \lambda_k \left(-\frac{N_k \lambda_k}{2} + \sum_{j=1}^{k} N_j \lambda_j \right)^2 \right) \tilde{E}_{bk}}{\left(2\sum_{k=1}^{P} N_k \lambda_k \right)^3}. \tag{A.66}$$

This equation thus provides an expression for the effective bending modulus of a multiply laminate in terms of the constituent materials and microstructural features, such as fibre radius and number of fibres in each ply.

References

Adams, D.F., Tsai, S.W., 1969. The influence of random filament packing on the transverse stiffness of unidirectional composites. J. Compos. Mater. 3 (3), 368–381.

Bažant, Z., Christensen, M., 1972. Analogy between micropolar continuum and grid frameworks under initial stress. Int. J. Solids Struct. 8 (3), 327–346.

Beveridge, A., Wheel, M., Nash, D., 2013. The micropolar elastic behaviour of model macroscopically heterogeneous materials. Int. J. Solids Struct. 50 (1), 246–255. https://doi.org/10.1016/j.ijsolstr.2012.09.023.

Bigoni, D., Drugan, W., 2007. Analytical derivation of Cosserat moduli via homogenization of heterogeneous elastic materials. J. Appl. Mech. 74 (4), 741–753.

Cosserat, E.M.P., 1970. Theory of deformable bodies. National Aeronautics and Space Administration.

Eringen, A.C., 1972. Nonlocal polar elastic continua. Int. J. Eng. Sci. 10 (1), 1–16.

Keane, A., Mccarthy, C., O'Dowd, N., 2008. The Effect of Matrix Non-linearity on the Properties of Unidirectional Composite Materials for Multi-Scale Analysis, vol. 88. doi:10.4203/ccp.88.312..

Lakes, R.S., 1983. Size effects and micromechanics of a porous solid. J. Mater. Sci. 18 (9), 2572–2580.

Lakes, R., 1995. Experimental methods for study of Cosserat elastic solids and other generalized elastic continua. Continuum models for materials with microstructure 70, 1–25.

Ma, H., Gao, X.-L., Reddy, J., 2011. A non-classical Mindlin plate model based on a modified couple stress theory. Acta Mech. 220 (1), 217–235.

Nourmohammadi, N., O'Dowd, N.P., Weaver, P.M., 2020. Effective bending modulus of thin ply fibre composites with uniform fibre spacing. Int. J. Solids Struct. 196–197, 26–40. https://doi.org/10.1016/j.ijsolstr.2020.04.004. URL: http://www.sciencedirect.com/science/article/pii/S0020768320301207.

Park, S.K., Gao, X.-L., 2006. Bernoulli-Euler beam model based on a modified couple stress theory. J. Micromech. Microeng. 16 (11), 2355–2359. https://doi.org/10.1088/0960-1317/16/11/015.

Wheel, M., Frame, J., Riches, P., 2015. Is smaller always stiffer? On size effects in supposedly generalised continua. Int. J. Solids Struct. 67–68, 84–92. https://doi.org/10.1016/j.ijsolstr.2015.03.026. URL: http://www.sciencedirect.com/science/article/pii/S0020768315001419.

Yang, J., Lakes, R.S., 1982. Experimental study of micropolar and couple stress elasticity in compact bone in bending. J. Biomech. 15 (2), 91–98.

Yang, F., Chong, A., Lam, D.C.C., Tong, P., 2002. Couple stress based strain gradient theory for elasticity. Int. J. Solids Struct. 39 (10), 2731–2743.